

**Fundamentals of High Temperature Processes**

**Effect of chlorine on the vaporization behavior of zinc and lead during high temperature treatment of dust and fly Ash**

Y.ZHANG *et al.*

Smelting process is a practical method to treat incineration ash of solid wastes in terms of volume reduction and decomposition/immobilization of toxic materials. In this process, chlorine is a key element to determine the removal ratio of heavy metals such as zinc and lead. The present paper is aiming to give a general review of researches on the effect of chlorine on the vaporization behavior of zinc and lead in molten slag. First, The basic information such as solubility/activity of chlorine in the slag, vaporization mechanism and kinetics relating to chlorides during heat treatment of fly ash are summarized. Then, the vaporization behaviors of zinc, lead and their chlorides during heating are discussed together with important process factors such as atmosphere, temperature, chemical composition and slag matrix. Further, some information on the oxychlorides of Zn and Pb are introduced.

(*cf. ISIJ Int.*, 44 (2004), 1457)

**Reduction of manganese oxides by methane-containing gas**

N.ANACLETO *et al.*

The paper presents results of reduction of pure manganese oxides by methane containing gas in non-isothermal and isothermal experiments and reduction mechanisms. The extent and rate of manganese oxide reduction were determined by on-line off-gas analysis using a mass-spectrometer in a fixed bed laboratory reactor in the temperature range 1 000–1 200°C at different gas compositions.

Manganese oxides were reduced to carbide Mn<sub>7</sub>C<sub>3</sub>. High extent and rate of reduction by methane-containing gas in comparison with carbothermal reduction were attributed to high carbon activity in the reducing gas, which was in the range 15–50 (relative to graphite). The rate of reduction of manganese oxide increased with increasing temperature. Increasing methane content in the reducing gas to 10–20 vol% CH<sub>4</sub> favoured the reduction process. Increase in hydrogen partial pressure had a positive effect on the reduction rate. Addition of carbon monoxide to the reducing gas retarded the reduction process. The addition of Fe<sub>3</sub>O<sub>4</sub> to manganese oxide increased the rate of reduction.

Reduction by methane-containing gas occurs through adsorption and cracking of methane with formation of active adsorbed carbon. Deposition of solid carbon retarded the reduction.

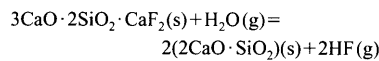
(*cf. ISIJ Int.*, 44 (2004), 1480)

**Determination of Gibbs energy of formation of cuspidine (3CaO·2SiO<sub>2</sub>·CaF<sub>2</sub>) by transpiration method**

H.FUKUYAMA *et al.*

The standard Gibbs energy change of the following reaction of cuspidine (3CaO·2SiO<sub>2</sub>·CaF<sub>2</sub>) with water vapor has been determined by a transpiration

method as



$$\Delta_r G^\circ / \text{kJ} = 265 - 0.116T (\pm 16) \\ (1\ 221 < T / \text{K} < 1\ 469)$$

From this result, the standard Gibbs energy of formation of cuspidine has been evaluated as,

$$\Delta_f G^\circ(\text{cuspidine}) / \text{kJ mol}^{-1} = -5\ 178 + 0.813T (\pm 19) \quad (1\ 221 < T / \text{K} < 1\ 469)$$

The constituent activities of the CaO–SiO<sub>2</sub>–CaF<sub>2</sub> system and fluorine emission from the system at elevated temperatures have been evaluated based on the obtained thermodynamic data.

(*cf. ISIJ Int.*, 44 (2004), 1488)

**Effect of P<sub>2</sub>O<sub>5</sub> addition on the rate of CO<sub>2</sub> dissociation on the surface of Fe<sub>3</sub>O<sub>4</sub>-base molten oxides**

H.MATSUURA *et al.*

For clarification of the surface active effect of P<sub>2</sub>O<sub>5</sub> in the reaction kinetics and mechanism of the various metallurgical processes, the effect of P<sub>2</sub>O<sub>5</sub> addition on the reaction rate of CO<sub>2</sub> dissociation on the surface of the Fe<sub>3</sub>O<sub>4</sub>, Fe<sub>3</sub>O<sub>4</sub>–CaO (mol%Fe<sub>3</sub>O<sub>4</sub>: mol%CaO=6:4), Fe<sub>3</sub>O<sub>4</sub>–SiO<sub>2</sub> (mol%Fe<sub>3</sub>O<sub>4</sub>: mol%SiO<sub>2</sub>=7:3), and Fe<sub>3</sub>O<sub>4</sub>–CaO–SiO<sub>2</sub> (mol%Fe<sub>3</sub>O<sub>4</sub>=35, mol%CaO/mol%SiO<sub>2</sub>=1.13–1.27 and 1.36–1.47) melts was investigated at 1 773 K with P<sub>CO<sub>2</sub></sub>/P<sub>CO</sub>=1 by using isotope exchange technique. The rate constant decreased with increasing P<sub>2</sub>O<sub>5</sub> content of melts and the residual rate constant was observed at high P<sub>2</sub>O<sub>5</sub> content. However, the change of the Fe<sup>3+</sup>/Fe<sup>2+</sup> ratio of molten oxide was not observed. Results were analyzed by using “site blockage model” of P<sub>2</sub>O<sub>5</sub>, and it was concluded that the rate controlling step of CO<sub>2</sub> dissociation was the dissociation reaction of adsorbed CO<sub>2</sub> molecule on the surface of molten oxides.

(*cf. ISIJ Int.*, 44 (2004), 1494)

**Ironmaking**

**The effect of BOF slag and BF flue dust on coal combustion efficiency**

L.S.ÖKVIST *et al.*

Injection into a BF of BOF slag to improve the slag formation and of BF flue dust to improve the recycling of in-plant fines has previously been tested. The effects on the PC combustion efficiency at different conditions, when these materials are co-injected with coal, have so far not been tested. Combustion efficiencies at varied temperature, O<sub>2</sub> enrichment, amount of PC, amount of added BOF slag or BF flue dust and particle size of the added material are measured in a fixed bed and a blowpipe model. The established facts that an increased temperature and O<sub>2</sub> enrichment or a decreased amount of coal increase the combustion efficiency are valid also when BOF slag or BF flue dust are added to the coal. By adjusting the combustion conditions, a decreased combustion efficiency can be counteracted, when a second material is co-injected with coal. The effect of BOF slag addition on coal combustion efficiency measured in the blowpipe model is insignificant, if a

fine fraction is used. The combustion efficiency is higher in the fixed bed compared with that in the blowpipe model. The addition of BF flue dust increases the combustion efficiency in the fixed bed.

(*cf. ISIJ Int.*, 44 (2004), 1501)

**Steelmaking**

**Evaluation of the energy developed by a multi-point side-wall burner-injection system during the refining period in a EAF**

C.MAPELLI *et al.*

An experimental activity has been performed to monitor the trend in slag–metal composition and temperature during the process of oxidation within an EAF system equipped by multi-burner injection system in which the injectors are distributed along the circumference of the furnace side-walls. This issue is a fundamental aspect to achieve a good balance for reaching the metallurgical goals and the energy savings necessary to maintain a good mix between the chemical specifications and the energy efficiency. The last aspect represents one of the most important bases to grant the competitiveness of the plant. A reliable interpretation of the data obtained from the industrial plant can also be evaluated through the use of the predictions performed by a developed simulation model.<sup>1)</sup>

(*cf. ISIJ Int.*, 44 (2004), 1511)

**Temperature prediction model for controlling casting superheat temperature**

N.GUPTA *et al.*

A temperature prediction model has been developed for controlling the casting superheat temperature. For ease of implementation, the model is intentionally made simpler having a combination of a one dimensional heat transfer model and a simple regression model. The model is based on the fact that the BOF temperature of the liquid steel along with the bath cooling behaviours controls the aimed casting superheat temperature. Starting with the steel liquidus temperature and calculating the required steel temperature backwards throughout the process line gives the targeted BOF tap temperature. The on-line picking up of actual data helps the model to predict for the next stage more accurately in forward direction. Based on the predicted steel temperature, plant operators can take any necessary corrective action like additional ladle heating and extra/reduced argon stirring to ensure the aim final ladle/tundish temperatures at the casting are achieved.

(*cf. ISIJ Int.*, 44 (2004), 1517)

**Casting and Solidification**

**Coordination environment of fluorine in the CaO–SiO<sub>2</sub>–CaF<sub>2</sub> Glasses bearing Na<sub>2</sub>O: A solid-state <sup>19</sup>F MAS NMR study**

M.HAYASHI *et al.*

The coordination environment of fluorine in the CaO–SiO<sub>2</sub>–CaF<sub>2</sub>–Na<sub>2</sub>O glasses has been measured by <sup>19</sup>F MAS NMR over a wide composition range including the similar compositions to those of

mould fluxes so as to determine the composition dependence of the coordination environment of  $F^-$ . Most of  $F^-$  are fourfold-coordinated by  $Ca^{2+}$  for the samples having the value of  $n_{Na}/(n_{Na}+n_{Ca}) \leq 0.3$ , where  $n$  represents the mole fraction of each cation. On the other hand, the samples having the value of  $n_{Na}/(n_{Na}+n_{Ca}) \geq 0.4$  contain  $F^-$  coordinated with both  $Na^+$  and  $Ca^{2+}$  and  $F^-$  sixfold-coordinated by  $Na^+$ .

(cf. *ISIJ Int.*, **44** (2004), 1527)

### Mathematical modeling of the tundish of a single-strand slab caster

R. PARDESHI *et al.*

The production of quality steel from a casting machine is dependent on a large number of inter-linked process parameters of ladle, tundish and casting operations. Continuous casting tundishes provide an important link between the ladle and the caster and the parameters of liquid metal in the tundish get affected by both up-stream and down-stream processes.

In this paper, the variation of tundish temperature under the influence of various operating parameters is numerically simulated using a mathematical model. A two-dimensional mathematical model, based on coupled fluid flow and heat transfer, is developed to simulate the tundish operation. The model accounts for turbulent fluid flow and dynamic level changes in the tundish. The model is validated with data published in the literature as well as with data obtained during the plant campaign. Simulation of the tundish operations demonstrates the capability of the model in capturing process dynamics correctly. The effect of a few important process parameters on the tundish outlet temperature is also studied.

(cf. *ISIJ Int.*, **44** (2004), 1534)

### Quality improvement of cast strip by temperature treatment of liquid metal

N. ZAPUSKALOV

The temperature at which a liquid metal is heated may be a source of variation in the quality of as-cast strips. The present study focuses on stabilization of the casting process and improving the quality of as-cast strip by temperature treatment of liquid metal.

At the condition of constant cooling rate it was found that the degree of melt overheating changes the characteristics of solidification as well as the as-cast properties. The phenomenon is interpreted from point of view of different structure of liquid metal at different temperature. At low degrees of overheating, solidification depends on the inherited interatomic structure from the solid state. At high degrees of overheating this inherited structure is destroyed and the melt becomes more homogeneous.

Typical and modified melting cycles were compared, to determine the influence of overheating on the as-cast strip quality. The modified cycle resulted in a more stable process and produced higher quality cast strip with better surface finish, a lower degree of segregation and less internal stress.

(cf. *ISIJ Int.*, **44** (2004), 1541)

## Chemical and Physical Analysis

### Roughness estimation of polycrystalline iron surface under high temperature by small glancing angle X-ray scattering

Y. FUJII *et al.*

Characterization of polycrystalline iron surfaces before and after baking at 500°C for 20 h in a vacuum of  $10^{-6}$  Pa is performed by small glancing angle X-ray scattering with use of a compact ultrahigh vacuum (UHV) X-ray diffractometer. A broadening of the scattered X-ray intensity profiles at a small glancing angle incidence of the X-ray appears on the baked specimen. The experimental results are compared with calculated simulation with some surface structure models, and show that the roughness of the surface after the baking is estimated to be about ten times of that before baking. This result is consistent with the result of AFM observation, and shows that glancing angle X-ray scattering with the use of a compact UHV X-ray diffractometer is a useful technique for non-destructive inspection of industrial material surfaces.

(cf. *ISIJ Int.*, **44** (2004), 1549)

### Forming Processing and Thermomechanical Treatment

#### Growth rate and phase composition of oxide scales during hot rolling of low carbon steel

V. V. BASABE *et al.*

The rate of scale growth on low carbon steel in air over the temperature range 600–1200°C and the phase composition changes that occur between 750–1200°C were investigated. The low carbon steel was oxidized with the air velocity of 4.2 cm/s in order to approximate the formation of secondary and tertiary scales in hot rolling. In addition, some experiments were performed with a lower air velocity of 0.14 cm/s. Above 1000°C, with the air velocity of 4.2 cm/s, a transition from a parabolic rate of oxidation to a linear rate of oxidation was observed as the temperature increased. This transition in oxidizing mechanisms was related to the porosity of the oxide scale. The phase composition of the oxide scales changed with temperature and time. For the initial 30 s of oxidation, wustite was the predominant phase in the temperature range 800–1200°C and as oxidation proceeded, the percentages of magnetite and hematite increased. The homogeneity of the oxide decreased as the oxidation temperature increased. At 850°C, with the air velocity of 4.2 cm/s, the oxide was homogeneous, and for the first 120 s of oxidation, the oxide had a high percentage of wustite and a low percentage of hematite. This indicates that 850°C is the ideal temperature for the finishing strip mill in order to reduce work roll wear and surface defects.

(cf. *ISIJ Int.*, **44** (2004), 1554)

## Transformations and Microstructures

### Crystallography and precipitation kinetics of copper sulfide in strip casting low carbon steel

Z. LIU *et al.*

Copper and sulfur are the major residual elements or impurities in scrap steel. The direct near net shape casting is an attractive process for scrap recycling. In the present paper, the precipitation and orientation relationship with matrix of copper sulfide in a strip casting steel were investigated by transmission electron microscopy. Nano-scale copper sulfides less than 50 nm with a face-centered cubic structure (Digenite) were found precipitating throughout the grains. These tiny copper sulfides have a cube-cube orientation relationship with the body-centered cubic  $\alpha$ -Fe matrix, which is  $(001)_{Cu_2S} // (001)_{\alpha-Fe}$  and  $[110]_{Cu_2S} // [110]_{\alpha-Fe}$ . Thermodynamic and kinetic analysis was conducted to compare the  $Cu_2S$  precipitation to the MnS precipitation in  $\gamma$ -Fe and  $\alpha$ -Fe. The calculation shows the nucleation of  $Cu_2S$  is dominant in the  $\gamma$ -Fe at low temperature and in the  $\alpha$ -Fe compared with that of MnS. The high cooling rate during strip casting and the complete coherent relationship with the matrix result in the present nano-scale copper sulfides.

(cf. *ISIJ Int.*, **44** (2004), 1560)

### Effects of boron, niobium and titanium on grain growth in ultra high purity 18% Cr ferritic stainless steel

E. EL-KASHIF *et al.*

Ultra-high purity 18% Cr ferritic stainless steel exhibits superior corrosion resistance. But, grain enlargement is likely to occur during their production and heat treatment, and this causes practical drawbacks in terms of surface qualities and mechanical properties. This study examines the effect of boron (B) addition on the grain growth of the ferritic stainless steel subjected to annealing after cold rolling. Since high Cr ferritic stainless steels often contain Nb or Ti, the effect of simultaneous addition of B with Nb or Ti is also examined as well as B single addition. It was found that B single addition retains grain growth after the recrystallization of the cold-rolled steel. The simultaneous addition of B and Nb leads to finer grain structure than Nb single addition, while the simultaneous addition of B and Ti leads to coarser grain structure than Ti single addition. When B is added with Nb, simultaneous precipitation of niobium carbide ( $Nb(C,B)$ ) and boron nitride (BN) was found, where NbC is refined by the B addition and the total density of the precipitates along with BN is increased as compared with that in only Nb added steel. When B is added with Ti, on the other hand, coarse  $M_{23}(C,B)_6$  was found to precipitate primarily on titanium nitride (TiN), and hence, the total density of the precipitates in Ti+B steel becomes lower than that in only Ti added steel which contains both TiN and titanium carbide (TiC). These grain structure development observed in the present study is explained primarily by the pinning effect of precipitates, and the precipitation behavior observed is found to be supported by thermodynamic calculation of phase

diagrams using Thermo Calc.

(cf. *ISIJ Int.*, **44** (2004), 1568)

### Behaviour of copper during high temperature oxidation of steel containing copper

*Y.KONDO*

It is well known that copper causes the hot shortness problem in steels and is a difficulty when using steel scrap in the steelmaking process. This is due to the property of copper enriching at the scale/metal interface and precipitating there as liquid during the high temperature oxidation of steels containing copper.

In this paper, the behaviour of copper during oxidation is investigated. A steel containing copper is oxidized and the distribution of copper in the scale is examined. It is found that copper is not only enriched at the scale/metal interface, but also exists in the upper magnetite ( $\text{Fe}_3\text{O}_4$ ) layer as a state of solid solution and along the grain boundaries of the wustite layer as a metal. From these results an assumption has been proposed that the liquid copper migrates from the scale/metal interface to  $\text{Fe}_3\text{O}_4$  layer along the grain boundaries.

Quantitative analysis revealed that the copper amount in the scale is greater than that at the scale/metal interface. Further analysis discovered that the amount of copper eliminated from the steel by oxidation is greater than the total amount of copper detected in the sample *i.e.* at the scale/metal interface, in the  $\text{Fe}_3\text{O}_4$  layer, and along the grain boundaries in the scale.

(cf. *ISIJ Int.*, **44** (2004), 1576)

### Kinetics and critical conditions for the initiation of dynamic recrystallization in 304 stainless steel

*G.R.STEWART et al.*

Commercial 304 austenitic stainless steel was deformed in compression at high temperatures (800 to 1280°C) and at strain rates from 0.001 to  $1 \text{ s}^{-1}$ . The critical and peak strains associated with dynamic recrystallization were determined based on changes in the work hardening rate as a function of the flow stress. The effect of the deformation variables ( $T$ ,  $\dot{\epsilon}$ ) on these values is analyzed; it is shown that over a range of temperature corrected strain rate ( $Z=10^{14}$

to  $10^{16} \text{ s}^{-1}$ ,  $Q_{\text{def}}=405 \text{ kJ/mol}$ ), the initiation of dynamic recrystallization is delayed. This retardation is attributed to the segregation of substitutional impurity elements, principally phosphorus, to the sub-boundaries of the newly-forming DRX grains.

(cf. *ISIJ Int.*, **44** (2004), 1581)

## Mechanical Properties

### Effects of Nb and Mo addition to 0.2%C–1.5%Si–1.5%Mn steel on mechanical properties of hot rolled TRIP-aided steel sheets

*S.HASHIMOTO et al.*

The development of high strength hot rolled TRIP (Transformation induced plasticity)-aided steel sheets with 780 MPa was carried out by taking into account the addition of Nb and Mo to 0.2C–1.5Si–1.5Mn mass% steel and coiling conditions after hot rolling. The results reveal that the addition of 0.05% Nb can attain higher elongation with higher strength compared with Nb-free steel. The obtained tensile strength in this steel was higher than 780 MPa. The multiple addition of 0.2% Mo with 0.05% Nb results in higher TS (Tensile Strength) by the large amount of fine NbMoC precipitates than Nb containing steel without the deterioration of TS–El (Elongation) balance under the possible hot rolling conditions. The good ductility in 0.05% Nb containing steel was mainly obtained by large volume fraction and high carbon concentration of retained austenite. In addition, finely dispersed retained austenite made some contribution to the improvement of ductility.

(cf. *ISIJ Int.*, **44** (2004), 1590)

### Artificial neural networks for modelling of the impact toughness of steel

*D.DUNNE et al.*

The application of artificial neural networks (ANNs) to the prediction of the Charpy impact toughness of quenched and tempered (QT) steels and ferrous weld metals is examined in detail. It is demonstrated that the Charpy impact toughness can be accurately predicted using the selected input variables and their ranges of values.

The capacity of ANNs to handle problems involv-

ing large sets of input variables is illustrated by a model developed to predict the impact energy of weld metal (WM) produced by flux cored arc welding (FCAW). The usefulness of ANNs for alloy design and process control is demonstrated through another model developed to predict the toughness of a QT structural steel as a function of composition and postweld heat treatment.

Although comparison of the two models indicates that the trends in toughness with changes in Mn and B concentrations are in opposite directions for weld metal and QT steel, it is shown that these trends can be reconciled with reported experimental results and theoretical interpretations.

(cf. *ISIJ Int.*, **44** (2004), 1599)

### Ductility of 0.1–0.6C–1.5Si–1.5Mn ultra high-strength TRIP-aided sheet steels with bainitic ferrite matrix

*K.SUGIMOTO et al.*

The effects of heat treatment and forming conditions on retained austenite characteristics and ductility of 0.1–0.6C–1.5Si–1.5Mn, mass%, ultra high-strength TRIP-aided sheet steels with bainitic ferrite matrix were investigated. These steels possessed large total elongations of about 20–25% in a tensile strength ranging from 700 to 1300 MPa when austempered at temperatures above martensite-start temperature ( $M_s$ ). The total elongations were enhanced by warm forming at two temperatures,  $T_{p1}$  and  $T_{p2}$ . The first peak forming temperatures  $T_{p1}$ s were between 0°C and 75°C and were nearly constant regardless of carbon content of the steels. This was associated with the strain-induced martensite transformation of a large amount of metastable retained austenite which suppressed a rapid fall of strain-hardening rate in an early strain range to resultantly increase the uniform and total elongations. On the other hand, the second peak forming temperatures  $T_{p2}$ s were between 200 and 300°C and further large total elongations beyond 30% were achieved in high carbon steels (0.4% C and 0.6% C steels) with tensile strength of 1300–1500 MPa. The large improvement was controlled by both the strain-induced bainite transformation and dynamic strain aging.

(cf. *ISIJ Int.*, **44** (2004), 1608)